Speed Control of Permanent Magnet Synchronous Motor by Anti windup PI Controller and Comparison with Fuzzy Controller

Maryam Imanzadeh
Department of Electrical Engineering
Ahar branch, Islamic Azad university, Ahar, Iran
maryam_imanzadeh2@yahoo.com

Adel Akbarimajd
Technical Engineering Department
University of Mohaghegh Ardabili, Ardabil, Iran
adelakbary@yahoo.com

ABSTRACT

In this paper, the driver with antiwindup and fuzzy high-performance and robust PI controller has been suggested for Permanent Magnet Synchronous Motor (PMSM). This controller is suggested for the design of the robust driver for three phase PMSM and the cost reduction of its control system. It's useful for the industrial application and automation and ultimately speed control and the improvement of the dynamic behavior of the PMSM. Antiwindup control strategy prevents the increase of the output beyond its saturation point. So, it avoids the saturation. In effect, the suggestion of this new speed control scheme is in line with a goal to realize a better antiwindup scheme. The simulation results are shown for PMSM for two cases of antiwindup control strategy and fuzzy control strategy and with different operation modes. For this purpose, different three phase PMSM output waveforms are presented. These waveforms are presented for fuzzy control strategy in constant torque, constant speed and different reference speeds with focus on speed curve, electromagnetic torque and phase currents.

Keywords

Permanent Magnet Synchronous Motor, speed control, antiwindup controller, fuzzy controller.

1. INTRODUCTION

Recently Vector-controlled Speed Adjustable drivers are adopted by the industry to meet the industrial requirements like quality and efficiency, higher speed control and fast response time. Conventional PI controllers simply can be used for the drive purposes, but all industrial processes are exposed to the certain limitations. For example, the analogue controllers can function in the limited range of the voltage and current and motor-driven actuator has a limited torque rate and speed. When they reach the limitation, if the controller is designed to work in the linear region, closed looped performance would deteriorate significantly compared to what expected. This deterioration process which is called integrator windup can significantly deteriorate the overshoot and the settling time. In practice integrator windup happens when the system has a large setpoint changes or big disturbances [1].

In recent decades, many control techniques have been proposed to develop different control schemes for the speed and torque in PMSM drivers. These schemes often can be categorized into vector control, Field oriented control, direct flux control and position sensorless control. Some of the research and papers about these control schemes for PMSM drivers are briefly introduced in [2-3].

In [4-5] a method is introduced for the estimation and speed control of PMSM with using sliding mode observer. In these papers, Lyapunov functions are chosen for determining the adaptive law for the speed and the stator resistance estimator. It seems that the conditions for converge cannot be simply guaranteed in the sliding mode. On the other hand, the integration of the rotor angular velocity can introduce too much error in the estimated angle of the rotor position. In general, the presence of the integrator in the controller can improve the steady state error, but it will slow down the system performance and makes the controller slow. A model-free predictive current control (PCC) is presented in [6] for improvement of the PMSM drive system in wide range of speed. Even though combining the feedforward current controlling compensator and flux-weakening algorithms can increase the capacity of IPM motor torque in the higher speeds, the overall effectiveness of these techniques depends on the accuracy of the motor parameters in the control function.

Torque ripple reduction for PMSMs by predictive direct torque control is presented in [7]. Direct torque control (DTC) for PMSMs got more attention compared to the conventional control methods because they don't have current controllers and fast dynamic response. But even with DTC techniques, big torque and stator flux ripples still remain in the system which create harmonics in the voltage and current of the stators in PMSMs. Maximum torque per ampere of stator current, above base speed, is analyzed in [8] with optimum alignment of the stator and magnet fields. With adjustment of the current angle, Operation at higher speeds with reduced torque can be achieved. This adjustment is for reducing the effective magnet flux (the equivalent of field weakening). Adaptive control of the surface mounted PMSM over its entire speed range is presented in [9]. The suggested adaptive flux weakening scheme can determine the right amount of d-axis current without the prior knowledge of load torque or inverter parameters.

A novel antiwindup strategy for PI speed controller is introduced in [10] to limit the unwanted side effect of the integrator windup at the time of large set-point changes. These unwanted side effects can also occur when the speed control mode is changed from P to PI control. This strategy assigns an appropriate initial value for the integrator. This value then can restrict the overshoot. One of the advantages of this proposed method is its independence of the operating condition. It guarantees the designed performance independent of the different set-point change and load torques. This strategy can be used easily in existing PI controllers.

In this paper, the performance of a linear controller based on antiwindup and nonlinear fuzzy drive system on PMSM is studied. The system modeling is presented in section two. The structure and the performance of the proposed scheme is presented in section three. The relations required for the design of the antiwindup controller is formulated in section four. The simulation results are presented in section five and finally the conclusion is drawn in section six.

2. PAPER SUBMISSION

In conditional integration, as shown in figure (1), the integration is switched on and off depending on certain conditions. With using conditional integration, it should be guaranteed that there is a zero steady state error. In addition to that, the integral term is only increased when certain conditions are satisfied, otherwise it is kept constant. Usually, when the controller is saturated, i≠i*, the integration is stopped.

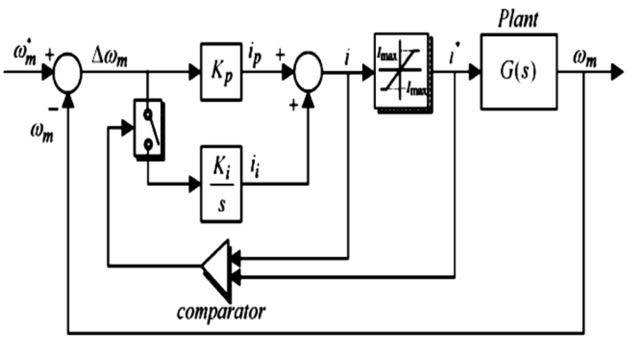

Figure 1. The block diagram schematic of the conditional integration

The proposed antiwindup scheme for current and speed control of PMSMs is based on the well-known conditional integral method. This integration can change under certain conditions between P and PI controller. However, the main difference is the way the initial value for the integration is set in PI controller. The ON-state and OFF-state switch, under certain conditions, can switch the controller to PI mode or P mode, respectively. The initial value (i_{i_0}) is loaded into the integrator in the P mode and PI controller when working in the PI mode uses this loaded value. The output value of the integrator is determined by i_{i_ss} to compensate for viscous damping and load torque. It should be at steady state condition without a speed error. Meanwhile, i_{i_0} is a pre-calculated integrator initial value. This value is passed through a low-pass filter (LPF) to prevent abrupt change in the current. The time constant of the filter should be fast enough to stabilize the changed value before the operation of the PI controller.

3. STRUCTURE AND PERFORMANCE OF THE PROPOSED SCHEME

The mechanical system is modeled as (1) where the K_T is motor torque constant and i(t) is a stator current.

$$J\frac{d\omega_m(t)}{dt}+B\omega_m(t)+T_L=K_T i(t) \quad (1)$$

PI controller model can be written as (2) where K_p is a proportional gain and K_i is an integral gain.

$$i(t)=i_p(t)+i_i(t), i_p(t)=K_p(\omega_m^*-\omega_m(t)), \frac{di_i(t)}{dt}=K_i(\omega_m^*-\omega_m(t)) \quad (2)$$

With plugging (2) into (1), the closed loop transfer function for speed can be derived by Laplace transformation as follows:

$$J(s\omega_m(s)-\omega_{m\_o})+B\omega_m(s)=K_T\left[\left(K_p+\frac{K_i}{s}\right)(\omega_m^*-\omega_m(s))+\frac{i_{i\_o}}{s}\right]-\frac{\tau_L}{s} \quad (3)$$

In the presented drive system, the load torque is assumed to be time-invariant and constant. it is $T_L(s)=\tau_L/s$ in Laplace and $\omega(s)$ is a Laplace transform of $\omega(t)$. When the controller enters the PI mode at $t=t_b$, the initial states value for speed and integrator term are shown by $\omega(t)=\omega_{m\_o}$ و $i_i(t_b)=i_{m\_o}$. in addition, (3) can be rewritten with considering the motor speed, the reference speed and the initial values assigned for the speed and the integrator terms as (4).

$$\omega_m(s)=\frac{K_T(K_p s+K_i)\omega_m^*-\tau_L+Js\omega_{m\_o}+K_T i_{i\_o}}{Js^2+(K_T K_p+B)s+K_T K_i} \quad (4)$$

In the steady state, $t=t_a$ before a new set-point change, the speed response can be denoted by $\omega_m(t_a)=\omega_m\_ss$ and the current can be denoted by $i_i(t_a)=\omega_{i\_ss}$. i_{i_ss} with constant load torque can be found as follows:

$$i_{i\_ss}=\frac{\tau_L+B\omega_{m\_ss}}{K_T} \quad (5)$$

At $t=t_b$, the P mode is changed to the PI mode. The initial integral value i_{i_0} can be defined by:

$$i_{i\_o}=\frac{\tau_L+B\omega_{m\_o}}{K_T}-K(\omega_m^*-\omega_{m\_o}) \quad (6)$$

It is worth to mention that the first right term in (6) shows the required current to operate at ω_{m_o} ,while the second right term can be assigned based on the initial value of the speed error required to reach the reference speed ω_m^* . A gain K can be designed to satisfy the antiwindup performance. The selection criteria will be discussed later. Plugging (6) into (4) gives:

$$\omega_m(s) = \frac{K_T[(K_p - K)s + K_i]\omega_m^* + (Js + K_T K + B)\omega_{m\_o}}{Js^2 + (K_T K_p + B)s + K_T K_i} \qquad (7)$$

The transfer function for the speed of PMSM finally can be rewritten during the PI mode with the initial state speed ω_{m_o}

$$\omega_m(s) - \frac{\omega_{m\_o}}{s} = H(s)\left(\omega_m^* - \frac{\omega_{m\_o}}{s}\right) \qquad (8)$$

If antiwindup gain $K=0$ and initial conditions are zero, the transfer function would equal to the original function, such as:

$$\omega_m(s) = \frac{K_T(K_p s + K_i)}{Js^2 + (K_T K_p + B)s + K_T K_i}\omega_m^* \qquad (9)$$

4. ANTIWINDUP CONTROLLER DESIGN

As explained in the final transfer function (8), the antiwindup gain K can improve the speed response characteristics in the PI mode. With assuming two poles, p_1 and p_2 and one zero, z_1, the system transfer function would be:

$$H(s) = -\frac{p_1 p_2}{z_1}\frac{(s - z_1)}{(s - p_1)(s - p_2)} \qquad (10)$$

where,

$$z_1 = -\frac{K_i}{K_p - K} < 0, p_1 = \frac{-(K_T K_p + B) + \sqrt{(K_T K_p + B)^2 - 4JK_T K_i}}{2J} < 0, p_2 = \frac{-(K_T K_p + B) - \sqrt{(K_T K_p + B)^2 - 4JK_T K_i}}{2J} < 0$$

Based on the introduced relations so far, the pole locations are determined by PI controller gains. However, the zero location is affected by the antiwindup gain and given PI gains. For example, if the zero be equal to the smaller pole, $z_1=p_1$ such as $|p_1|<|p_2|$, then the antiwindup gain will become like $K=K_p+K_i/p_1$. With this gain, (10) can be simplified as:

$$H(s) = \frac{-p_2}{s - p_2} \qquad (11)$$

So, (11) is an equation of a first-order low pass filter without an overshoot. If the windup gain is smaller than the specified one, then a higher overshoot will be reached. Meanwhile, a larger K results in a slower response. The relationship at the boundary condition of the P to the PI mode transition can be used to calculate the initial current and speed condition. The controlled current output, if assumed to be same as the limited current, gives:

$$i_{i\_o} + K_p(\omega_m^* - \omega_{m\_o}) = \pm I_{\max} \qquad (12)$$

The maximum limited current is shown with $+I_{max}$, while the minimum limited current is shown with $-I_{\max}$. Using (6) and (12), the initial current of the integrator is calculated:

(13)

$$i_{i\_o} = \frac{K_p(\tau_L + B\omega_m^*) - (K_T K + B)I_{\max}}{K_T(K_p - K) - B} \quad , \qquad i \geq 0$$

$$i_{i\_o} = \frac{K_p(\tau_L + B\omega_m^*) + (K_T K + B)I_{\max}}{K_T(K_p - K) - B} \quad , \qquad i < 0$$

Moreover, the load torque can be expressed as $\tau_L=K_T i_{i\_ss}-B\omega_{m\_s}$ based on the condition that the system is controlled at speed ω_{m_ss} and the current i_{i_ss}. equation (13) can be rewritten as (14) with the known values.

(14)

$$i_{i\_o} = \frac{K_p(K_T i_{i\_ss} + B(\omega_m^* - \omega_{m\_ss})) - (K_T K + B)I_{\max}}{K_T(K_p - K) - B} \quad , \qquad i \geq 0$$

$$i_{i\_o} = \frac{K_p(K_T i_{i\_ss} + B(\omega_m^* - \omega_{m\_ss})) + (K_T K + B)I_{\max}}{K_T(K_p - K) - B} \quad , \qquad i < 0$$

During the saturation mode (P mode), the initial current of the integrator is passed through a low pass filter with transfer function of $PF=\omega_c/(s+\omega_c)$ at a fast range to reach a steady state before initiating PI control mode. The initial speed is given by the following relation:

(15)

$$\omega_{m\_o} = \frac{K_T(K_p - K)\omega_m^* + \tau_L - K_T I_{\max}}{K_T(K_p - K) - B} = \frac{K_T(K_p - K)\omega_m^* - B\omega_{m\_ss} + K_T(i_{i\_ss} - I_{\max})}{K_T(K_p - K) - B} \quad , \qquad i \geq 0$$

$$\omega_{m\_o} = \frac{K_T(K_p - K)\omega_m^* + \tau_L + K_T I_{\max}}{K_T(K_p - K) - B} = \frac{K_T(K_p - K)\omega_m^* - B\omega_{m\_ss} + K_T(i_{i\_ss} + I_{\max})}{K_T(K_p - K) - B} \quad , \qquad i < 0$$

In practice, the motor has a relatively low viscous damping coefficient, i.e, ($B\approx 0$) or viscous damping is only a very small percentage of the total load torque, i.e. $B\omega_m << \tau_L$. so, the initial values of current and speed can be presented with simpler equations of (16) and (17).

$$i_{i\_o} \approx \frac{K_p(\tau_L / K_T) - KI_{\max}}{K_p - K} = \frac{K_p i_{i\_ss} - KI_{\max}}{K_p - K} \quad , \qquad i \geq 0$$

$$i_{i\_o} \approx \frac{K_p(\tau_L / K_T) + KI_{\max}}{K_p - K} = \frac{K_p i_{i\_ss} + KI_{\max}}{K_p - K} \quad , \qquad i < 0$$

(16)

$$\omega_{m\_o} \approx \omega_m^* + \frac{\tau_L - K_T I_{\max}}{K_T(K_p - K)} = \omega_m^* + \frac{i_{i\_ss} - I_{\max}}{K_p - K} \quad , \qquad i \geq 0$$

$$\omega_{m\_o} \approx \omega_m^* + \frac{\tau_L + K_T I_{\max}}{K_T(K_p - K)} = \omega_m^* + \frac{i_{i\_ss} + I_{\max}}{K_p - K} \quad , \qquad i < 0$$

(17)

The simulated block diagram schematic for the proposed PMSM antiwindup drive system with the initial values for current and speed according to (16) and (17) is shown in figure (2). According to this figure and as explained earlier, during the controller windup which is determined by motor current, the controller switches between PI control mode to P control mode with one switch. The proposed antiwindup strategy can be applied to the PI controllers. For the realization of this control scheme, at first the non-zero initial values for motor current and speed should be calculated with using a transfer function. Then one low pass filter for the reduction or remove of the overshoot in the drive system speed response should be designed. This filter can be designed using a transfer function taking derivative from the system poles and zeros.

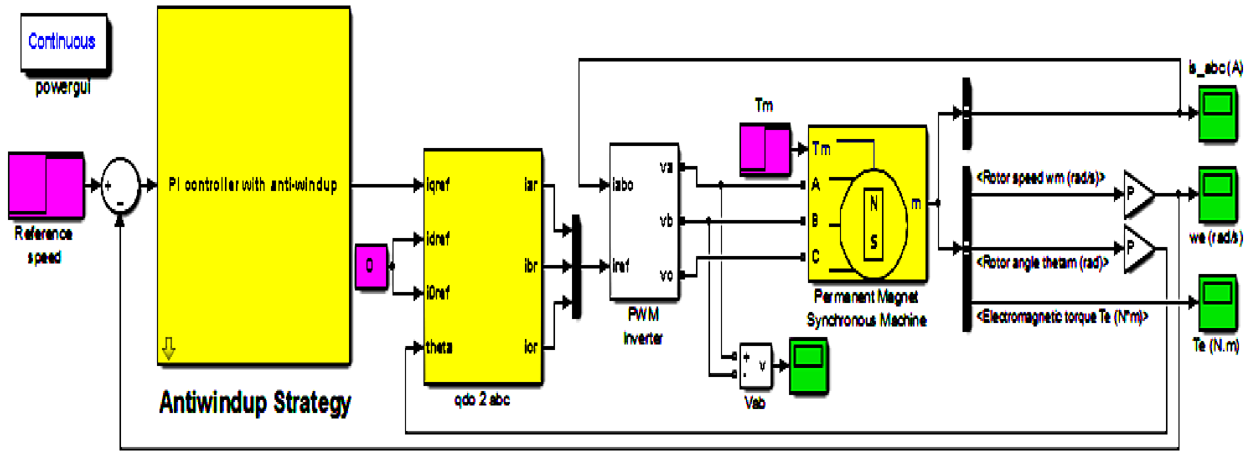

Figure 2. The drive system block diagram with antiwindup controller

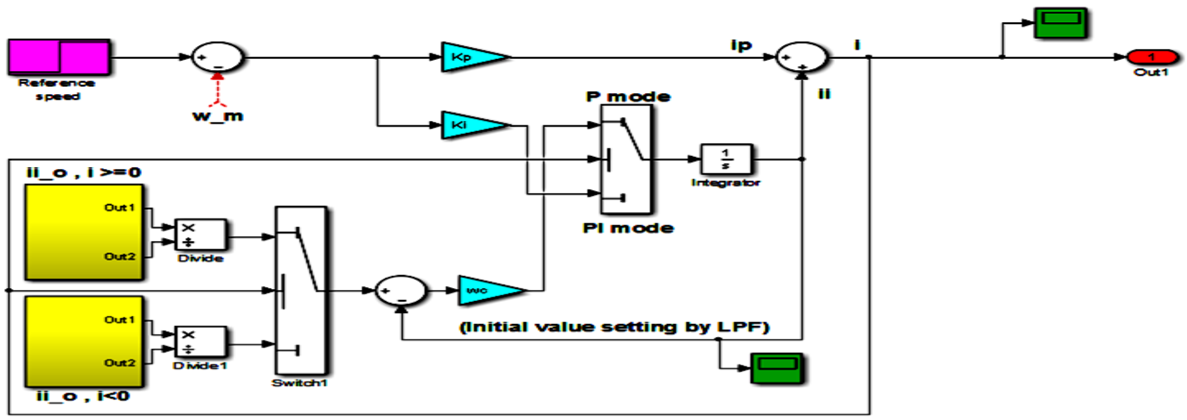

Figure 3. Block diagram of the antiwindup controller

5. SIMULATION RESULTS

The structure and the relations of PMSM drive system and also the proposed control system are fully explained and analyzed in the previous sections. In this section, first the block diagram schematics of PMSM drive system simulated by the electrical and dynamic equations, is presented. Then, the simulation studies of the drive system are performed within Matlab/Simulink environment and the results, waveforms and the graphs are presented.

5.1 The simulated model of the PMSM drive system

For finding the characteristics of the PMSM motor and its drive system, at first, the motor should be modeled. PMSM modeling comprises two parts: electrical and mechanical. The first part calculates the currents and the electromagnetic torque of the motor. For calculating the currents, the counter electromotive forces should be calculated. As expressed, these forces have three phase sinusoidal waveforms with 120 degree phase difference. The overall block diagram schematic for PMSM drive system is shown in figure (2). PMSM motor characteristics used for the simulation is listed in table (1).

Table 1. Parameters of the PMSM motor and its drive system

Parameter	Value
Phase inductance (*mH*)	8.5
Inertia ($kg.m^2$)	0.0000321
Nominal speed (*rad/sec*)	2000
Phase resistance (Ω)	2.875
Polepairs	4
Torque constant factor (*V/rad/sec*)	0.3252

In this section, the simulation results of the drive system with the fuzzy speed control are presented. Figure (3) shows the waveforms of speed, phase currents and three phase PMSM electromagnetic torque with using fuzzy control strategy. As shown in this figure, phase currents are sinusoidal and have fluctuations and ripples. Phase current ripples are because of the commutation region of the drive system inverter switches. These inverter switches have unequal ON and OFF time intervals during one cycle. These ripples in phase currents cause the fluctuations in the motor torque. But the ripples in the current and torque in this case are smaller than the case with the control system without antiwindup strategy.

As shown in figure (3), the motor speed reference is 500 rad/s till 0.5 sec and then it will increase to 1500 rad/s. the load torque is constant and equal to 20 N.m. according to figure (3-a) , the motor speed follows the speed reference but in this case the rising time of the motor speed is so much better than the control system without antiwindup strategy. In this case, the rising time is equal to 0.1 sec. however the overshoot is zero with fuzzy control system and the speed response have zero steady state error. According to (3-b), when the speed reference at time 0.5 sec changed, the motor output torque is increased significantly and then settle back to its reference position. The jump magnitude in this case is about two times of the jump magnitude in the control system without antiwindup strategy.

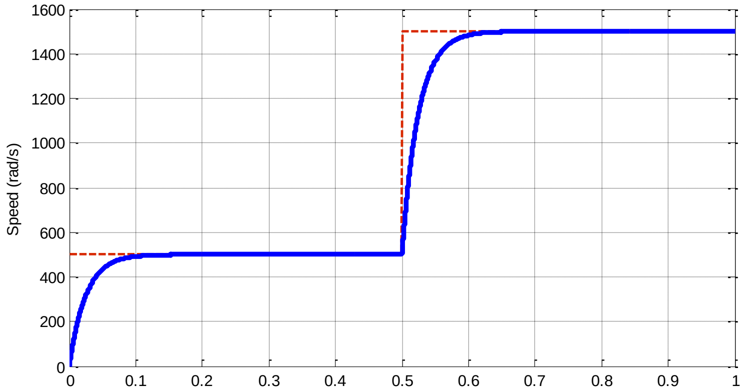

a. Seed curve

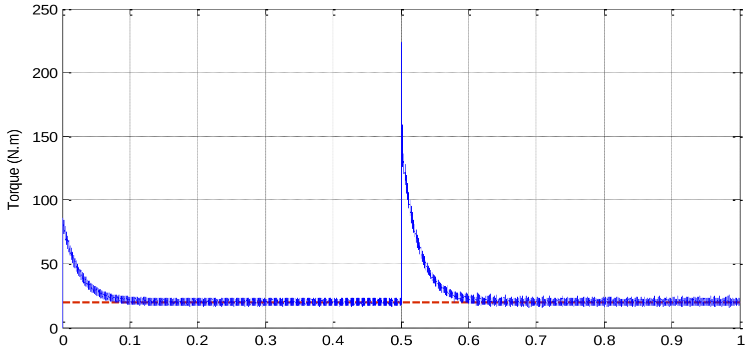

b. Electromagnetictorque

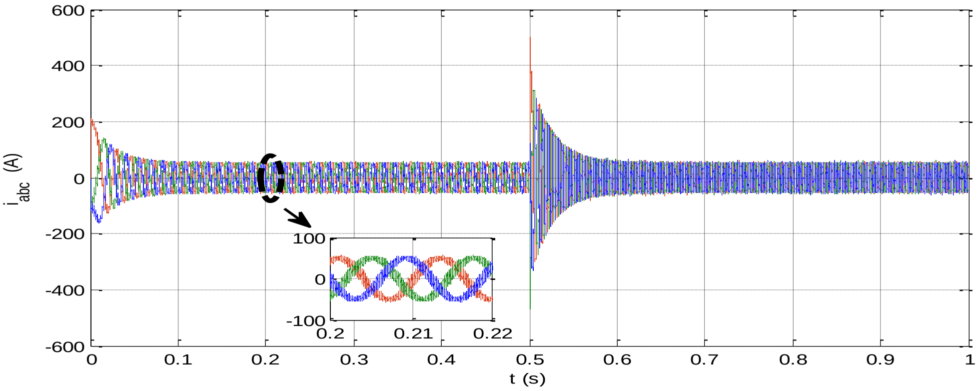

c. Phase currents

Figure 3. The PMSM three phase output waveforms with fuzzy control strategy with the constant load torque

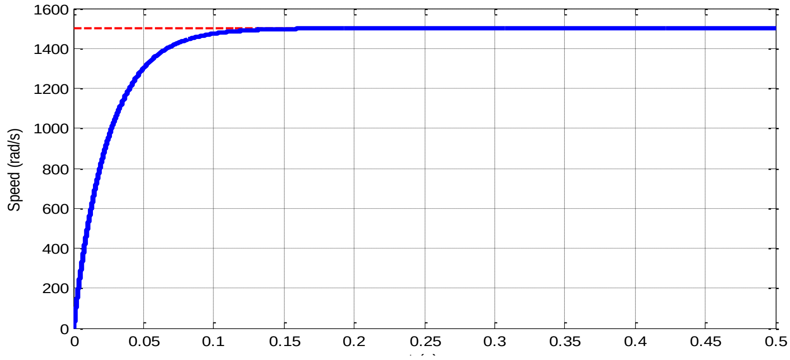

a) Speed curve

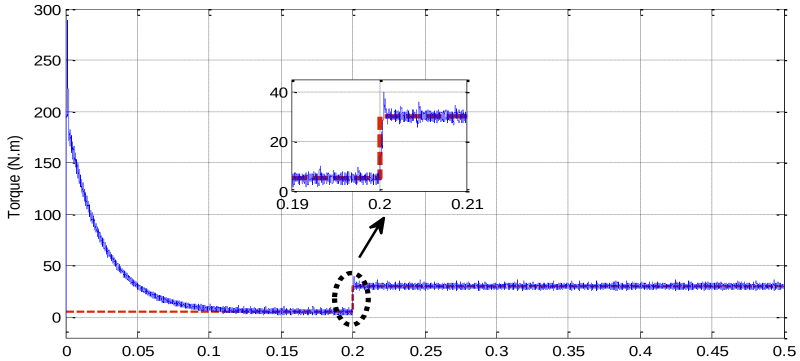

b) Electromagnetic torque

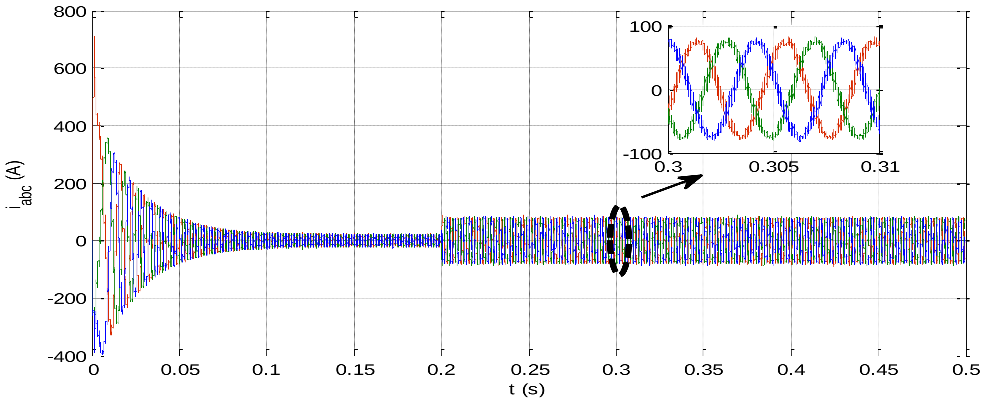

c) phase currents

Figure 4. Three phase PMSM output waveforms with the fuzzy control strategy for the constant speed

In figure (4), PMSM works with the constant speed and varying load torque. Load torque is equal to 5 N.m till 0.2 sec but it will increase to 30 *N.m* afterwards. According to (6-4-b), the torque ripple and fluctuations till 0.2 *sec* (in smaller loads) are almost equal to the ripple and fluctuations in higher value of loads (30 *N.m*). it shows the robustness of the fuzzy control strategy to antiwindup controller. After 0.2 *sec*, the load is increased and the motor response to different speed references and the output signal of the fuzzy control during the speed changes are shown in figure (5).

As shown in the figure, the motor output signal is increased as soon as the increase in the speed references and following motor speed response. Since the fuzzy controller is a nonlinear and intelligent controller, it responds quickly to the changes and dampen the increase in the controller output signal. According to (5-b), fuzzy controller output signal during the changes in the speed at 0.4 sec in the normal mode of the drive system and the constant speed is 50. During the speed error, this value increases to 200 (4 times). However this value is still low compared to the windup in the antiwindup controller and it won't make this system saturated.

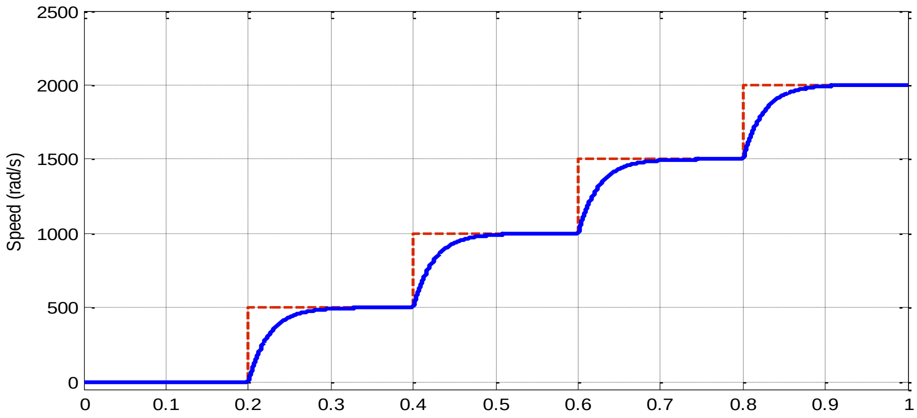

a) Speed curve

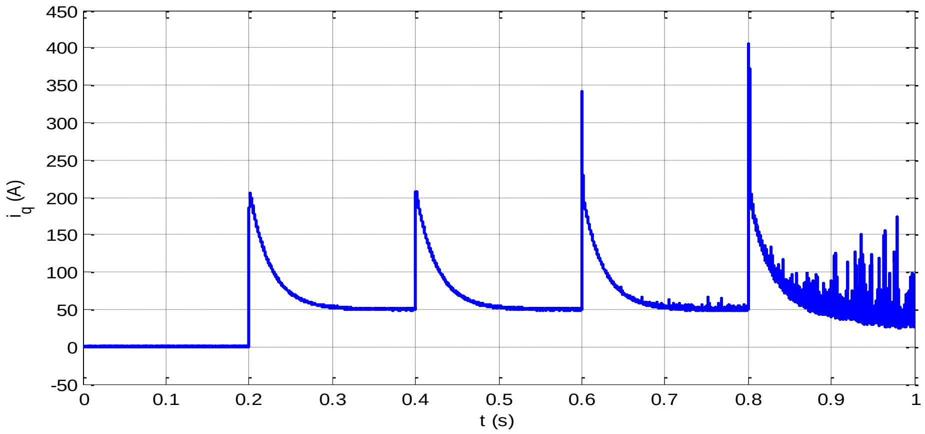

b) Controller output signal (torque component)

Figure 5. Three phase PMSM output waveforms with the fuzzy control strategy for the varying speed

5.2 Comparison of the performance of the fuzzy and antiwindup controller

According to the figure (6) the motor speed input is variable. Zero, half of the nominal value and the nominal value (2000 *rad/s*) are selected for its value.

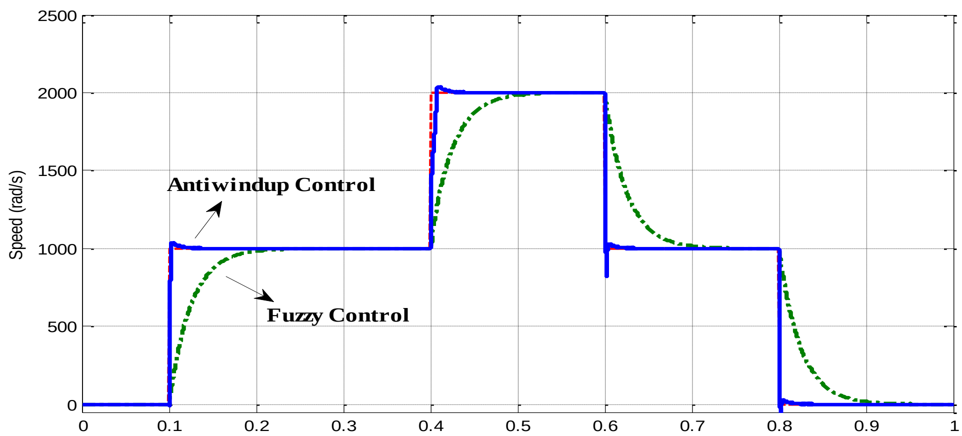

a) Speed curve

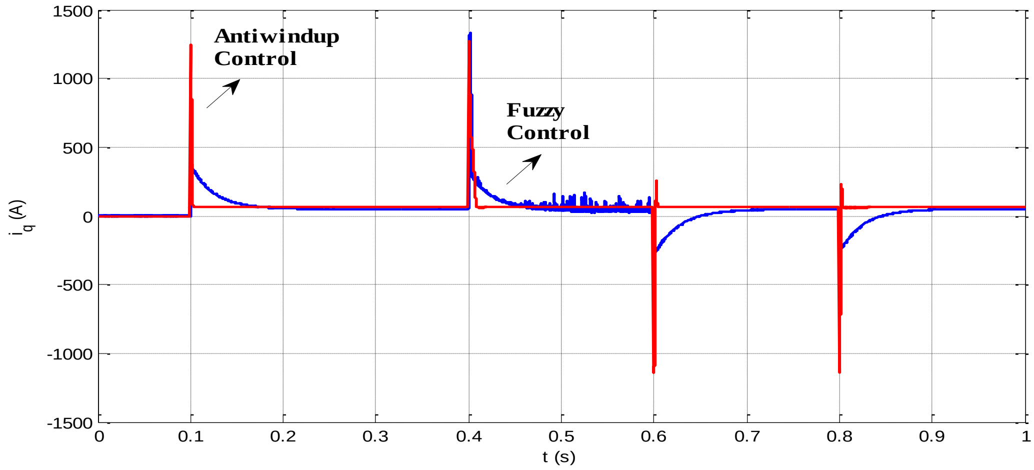

b) Controller output signal

Figure 6. Comparison of the performance of the fuzzy and antiwindup controller

6. CONCLUSION

In this paper, the drive system with antiwindup and fuzzy high-performance and robust PI controller has been suggested for Permanent Magnet Synchronous Motor (PMSM). The antiwindup strategy restricts the controller output value not to let it overreach to the saturation region. As shown with the simulation results, during the increase in the speed reference or motor load, the antiwindup controller shift to P mode operation and prevent the windup. On the other hand, another controller based on the fuzzy logic is introduced for PMSM which is a nonlinear and intelligent controller. Fuzzy control while increasing the overshoot time, has zero overshoot. It has a lower torque ripple than the antiwindup strategy. Compared to the antiwindup controller, it has a slower speed response and is sluggish. However, the motor drive system response to the speed changes or load changes are better in the fuzzy control strategy than the antiwindup. Compared to the traditional choice of the controller for PMSM, the proposed drive system are cheaper and the costs associated with the complicated hardwares for controller realization are removed. This drive system improve the performance of the driver torque. However, the fuzzy controller as motor speed controller is used for improvement of the dynamic response and the decrease of the motor steady state error. The simulation results of the proposed drive system for the verification of the better performance of motor and its drive system is run in MATLAB software for different operation modes.

REFERENCE

1. Bohn, C. & Atherton, D.P. (1995). An analysis package comparing PID antiwindup strategies, IEEE Control Syst. Mag., vol. 15, no.2, pp.34-40.
2. Chou, M.C., Liaw, C.M., Chien, S.B., Shieh, F.H., Tsai, J.R., & ChangH.C. (2011). Robust Current and Torque Controls for PMSM Driven Satellite Reaction Wheel, IEEE Trans. Aerospace and Electronic Systems, vol. 47, no.1, pp. 58-74.
3. Inoue, Y., Morimoto, S., & Sanada, M. (2012). Comparative Study of PMSM Drive Systems Based on Current Control and Direct Torque Control in Flux-weakening Control Region, IEEE Trans. Ind. Appl., vol. 48, no.6, pp. 2382-2389.
4. HanY.S., Choi J.S. & KimY.S., (2000). Sensorless PMSM drive with a sliding mode control based adaptive speed and stator resistance estimator, IEEE Trans. Magnetics, vol. 36, pp. 3588-3591.
5. Elbuluk, M., & Li, C. (2003). Sliding mode observer for wide-speed sensorless control of PMSM drives, in Conf. Rec. IEEE-IAS Annual Meeting, vol. 1, pp. 480-485.
6. Lin, C.K., Liu, T.H., Yu, J.T., Fu, L.C., & Hasiao, C.F. (2014). Model-Free Predictive Current Control for Interior Permanent-Magnet Synchronous Motor Drives Based on Current Difference Detection Technique, IEEE Trans. Ind. Electron., vol. 61, no.2, pp. 667-681.
7. preindl M., & Bolognani, S., (2013). Model Predictive Direct Torque Control With Finite Control Set for PMSM Drive Systems, Part 2: Field Weakening Operation, IEEE Trans. Ind. Info., vol. 9, no.2, pp. 648-657.
8. Sebastian, T., & Slemon, G.R. (1986). Operating limits of inverter-driven permanent magnet motor drives, IEEE Trans. Inds. Appl., vol. 23, no.2, pp. 800-805.
9. SozerY.& TorreyD.A., (1998). Adaptive Flux weakening control of permanent magnet synchronous motors, in Conf. Rec. IEEE-IAS Ann. Meet., vol. 1, pp. 475-482.
10. Choi, J.W., & Lee, S.C. (2009). Antiwindup Strategy for PI-Type Speed Controller, IEEE Trans. Ind. Electron., vol. 56, no.6, pp. 2038-2046.
11. Nasar, S.A., Boldea, I., & Unnewehr, L. (1993). Permanent magnet, reluctance and self-synchronous motors, CRC Press, Florida,.
12. Zhu, H., Xiao, X., & Li, Y. (2012). Torque Ripple Reduction of the Torque Predictive Control Scheme for Permanent-Magnet Synchronous Motors, IEEE Trans. Indsl Electrs, vol. 59, no.2, pp. 871-877.
13. Inoue, Y., Morimoto, S., & Sanada, M., (2009). A novel method of maximumpower operation for IPMSMs in DTC system, Proceedings of the 13th European Conference on Power Electronics and Applications (EPE 2009), pp.1-8